

# Supplementary Material for “Computational Study of the Mixed B-site Perovskite $\text{SmB}_x\text{Co}_{1-x}\text{O}_{3-\delta}$ ( $\text{B}=\text{Mn, Fe, Ni, Cu}$ ) for Next Generation Solid Oxide Fuel Cell Cathodes.”

*Emilia Olsson,<sup>1</sup> Jonathon Cottom,<sup>2</sup> Xavier Aparicio-Anglès,<sup>1</sup> and Nora H. de Leeuw<sup>1,3\*</sup>*

<sup>1</sup> Department of Chemistry, University College London, WC1H 0AJ, London, United Kingdom

<sup>2</sup> Department of Physics and Astronomy, University College London, WC1H 0AJ, London, United Kingdom

<sup>3</sup> School of Chemistry, Cardiff University, Main Building, Park Place, CF10 3AT, Cardiff, United Kingdom

The Electronic Supporting Information (ESI) contains a summary of the interatomic potential parameters used for the calculation of thermal expansion coefficients (Table S1), a graphical representation of the different magnetic structures investigated in the main article (Figure S1), a description on how to obtain chemical potential phase diagrams and link this to the oxygen vacancy formation energy; chemical potential phase diagrams for  $\text{SmMnO}_3$  and  $\text{SmFeO}_3$  (Figure S2); a complete list of all the differences in energy between the different dopant configurations in the individual systems (Table S2); the B-O bond lengths for the most stable structures (Table S3); Bader charges for  $\text{SmB}_x\text{Co}_{1-x}\text{O}_3$  (Table S4), the magnetic structures calculated for  $\text{SmBO}_3$  and their relative energies (Table S5); larger DOS (Figure S3-S7), and electrical conductivities for all systems (Table S6). Additionally, a table with all the oxygen vacancy positions and oxygen vacancy formation energies is included in Table S7, and thermal expansion coefficients in Table S8.

## Force Field Parameters

**Table S1.** Interatomic potential parameters for  $\text{SmB}_x\text{Co}_{1-x}\text{O}_3$ . Potential cutoff set to 12 Å.

Interaction	Short range interactions			Shell Model			
	A (eV)	$\rho$ (Å)	C (eVÅ <sup>6</sup> )	Y (e)	k (eVÅ <sup>-2</sup> )	ref	
<b>Sm<sup>3+</sup>-O<sup>2-</sup></b>	1252.94	0.3590	0.00	<b>Sm<sup>3+</sup></b>	-0.250	173.90	<sup>1</sup>
<b>Co<sup>3+</sup>-O<sup>2-</sup></b>	1329.82	0.3087	0.00	<b>Co<sup>3+</sup></b>	2.040	196.30	<sup>2</sup>
<b>O<sup>2-</sup>-O<sup>2-</sup></b>	22764.30	0.1490	43.00	<b>O<sup>2-</sup></b>	-2.389	42.00	<sup>2</sup>
<b>Fe<sup>3+</sup>-O<sup>2-</sup></b>	1156.36	0.3299	0.00	<b>Fe<sup>3+</sup></b>	4.97	304.7	<sup>2</sup>
<b>Mn<sup>3+</sup>-O<sup>2-</sup></b>	1267.50	0.3214	0.00	<b>Mn<sup>3+</sup></b>	3.00	95.0	<sup>2</sup>
<b>Ni<sup>3+</sup>-O<sup>2-</sup></b>	1947.47	0.2882	0.00	<b>Ni<sup>3+</sup></b>	3.344	193.7	
<b>Cu<sup>3+</sup>-O<sup>2-</sup></b>	5888.83	0.2427	0.00	<b>Cu<sup>3+</sup></b>	4.00	99.0	

## Schematic of Magnetic Structures

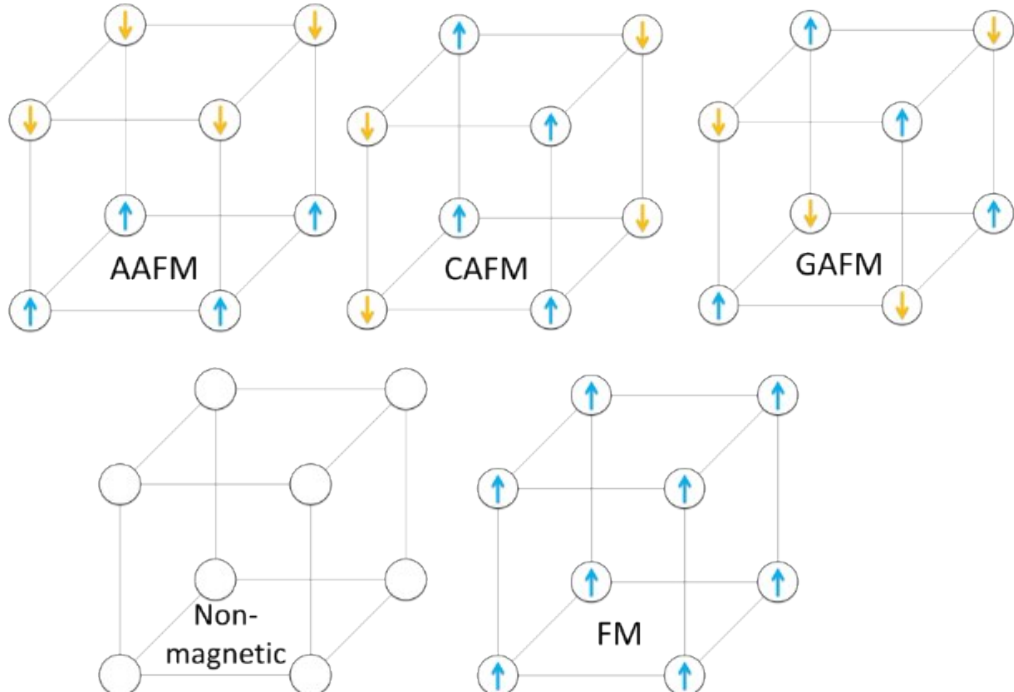


**Figure S1.** Schematic representation of potential magnetic structures. For simplicity, each sphere represents a Co or B atom (dependent on system and configuration). Yellow downwards pointing arrows represent  $\beta$  alignment, whereas blue upwards arrows are  $\alpha$  alignment.

## Chemical Potentials and Oxygen Vacancy Formation Energy

The range for which  $\mu_o$  equation 4 is stable can be linked to the chemical potential phase diagram for its specific  $\text{SmBO}_3$ . For  $\text{SmBO}_3$ , the chemical potentials must satisfy the following condition:

$$g_{\text{SmBO}_3}^{\text{bulk}} = \mu_{\text{Sm}} + \mu_B + 3 \cdot \mu_O \quad (\text{S.1})$$

where  $g_{\text{ABO}_3}^{\text{bulk}}$  is the free energy per formula unit for bulk  $\text{SmBO}_3$ , and  $\mu_i$  is the chemical potential of each species. To avoid the formation of elementary crystals, each  $\mu_i$  must fulfil:

$$\Delta\mu_{\text{Sm}} = \mu_{\text{Sm}} - g_{\text{Sm}}^{\text{bulk}} \leq 0 \quad (\text{S.2})$$

$$\Delta\mu_B = \mu_B - g_B^{\text{bulk}} \leq 0 \quad (\text{S.3})$$

$$\Delta\mu_O = \mu_O - \frac{1}{2}g_{\text{O}_2}^{\text{tot}} \leq 0 \quad (\text{S.4})$$

where  $\Delta\mu_i$  is the chemical potential deviation,  $g_i^{\text{bulk}}$  is the free energy of  $i$ , and  $g_{\text{O}_2}^{\text{tot}}$  is the free energy of  $\text{O}_{(g)}$ . It is widely accepted that  $g_{\text{O}_2}^{\text{tot}}$  can be approximated by the electronic DFT energy of  $\text{O}_{(g)}$  ( $E_{\text{O}_2}$ ).<sup>3</sup> This approximation is made under the assumption that the bulk is in thermodynamic equilibrium with the surface, and the latter is in equilibrium with the gas phase.

Under oxygen-rich conditions,  $\mu_o$  will be determined from equation S.4 when  $\mu_o$  is at a

maximum, i.e.  $\mu_o = \frac{1}{2}E_{\text{O}_2}$ . Under oxygen-poor conditions, it will be determined by the formation of the elementary crystals Sm and B respectively. In this context, S.1 can be rewritten as:

$$\mu_O \geq \frac{1}{3} \left[ g_{\text{SmBO}_3}^{\text{bulk}} - g_{\text{Sm}}^{\text{bulk}} - g_B^{\text{bulk}} \right] \quad (\text{S.5})$$

and then, the limit for the oxygen-poor situation is

$$\frac{1}{3}\Delta G_{\text{ABO}_3}^f \leq \Delta\mu_O \leq 0 \quad (\text{S.6})$$

where  $\Delta G_{\text{ABO}_3}^f = \left[ g_{\text{ABO}_3}^{\text{bulk}} - g_A^{\text{bulk}} - g_B^{\text{bulk}} - \frac{3}{2}E_{\text{O}_2} \right]$ .

The precipitation of intermediate oxides, *e.g.*  $\text{AO}_2$ , is considered through their formation free energy:

$$\Delta G_{\text{AO}_2}^f > \Delta\mu_A + 2\Delta\mu_O \quad (\text{S.7})$$

Solving the set of inequalities, a range for chemical potentials is obtained in which the investigated perovskites are stable and phase diagrams may be constructed. It is worth noting that throughout this work, we considered  $\mu_o$  and  $\mu_{\text{Sm}}$  as independent variables, whereas  $\mu_B$  is dependent on these.

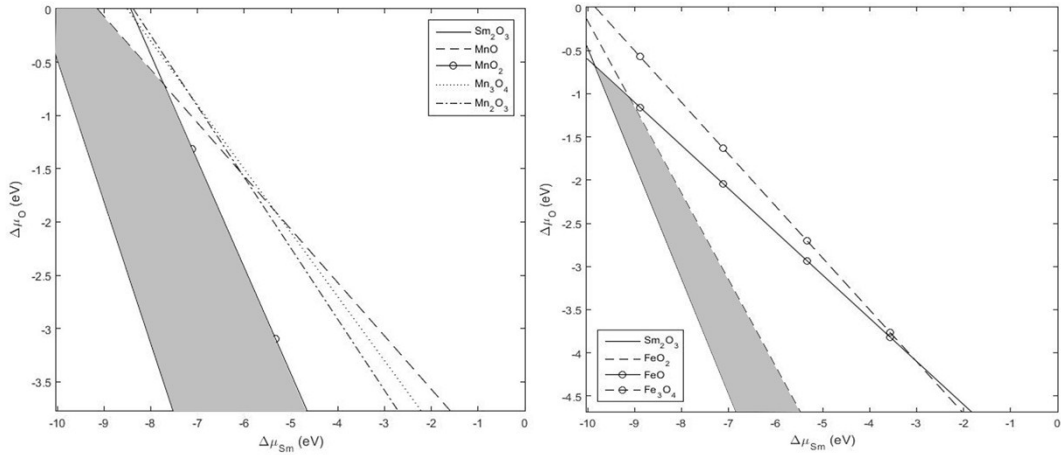


Figure S2. Chemical potential phase diagrams of  $\text{SmMnO}_3$  (left) and  $\text{SmFeO}_3$  (right). For  $\text{SmCoO}_3$  phase diagram, please see Olsson *et al.*<sup>4</sup>

### Energetic Evaluation of Dopant Configuration

Table S2. Energy difference (in eV per 2x2x2 simulation cell) between different dopant configurations. x=0.125 is not included as it only has 1 possible inequivalent configuration.

	<b>Conf. No.</b>	<b>Mn</b>	<b>Fe</b>	<b>Ni</b>	<b>Cu</b>
<b>x=0.25</b>	1	0.00	0.00	0.00	0.00
	2	0.56	0.43	0.41	0.10
	3	0.97	0.68	0.50	0.38
<b>x=0.50</b>	1	0.00	0.00	0.00	0.00
	2	0.27	0.84	0.43	0.14
	3	0.30	0.85	0.85	0.23
	4	0.30	1.30	0.91	0.32
	5	0.36	1.34	1.15	0.50
	6	0.47	1.59	1.96	1.48
<b>x=0.75</b>	1	0.00	0.00	0.00	0.00
	2	0.11	0.26	1.00	0.40
	3	0.16	0.43	2.23	0.52

### Structural Properties of $\text{SmB}_x\text{Co}_{1-x}\text{O}_3$

Table S3. B-O bond lengths ( $\text{\AA}$ ) in  $\text{SmB}_x\text{Co}_{1-x}\text{O}_3$ . Co-O in  $\text{SmCoO}_3$  is 1.88  $\text{\AA}$ .

<b>B</b>	<b>x=0.125</b>	<b>x=0.25</b>	<b>x=0.5</b>	<b>x=0.75</b>	<b>x=1.00</b>
<b>Mn</b>	Mn-O 1.90	1.89, 1.91	1.88, 1.91, 1.93, 1.94	1.90, 1.92, 1.95, 1.96	1.94
	Co-O 1.87, 1.88, 1.89	1.87, 1.89	1.88, 1.90, 1.94, 1.95	1.88, 1.89	
<b>Fe</b>	Fe-O 1.90	1.92, 1.93	1.94	1.93, 1.95, 1.96, 1.97	1.94
	Co-O 1.86, 1.88, 1.89	1.85, 1.86, 1.88, 1.89, 1.90	1.87	1.88, 1.89	
<b>Ni</b>	Ni-O 1.93	1.93, 1.94	1.91, 1.93	1.92, 1.93, 1.94	1.88
	Co-O 1.86, 1.88, 1.91, 1.93	1.84, 1.87, 1.88, 1.89, 1.90	1.84, 1.91	1.83, 1.87	
<b>Cu</b>	Cu-O 1.90	1.89, 1.96	1.89, 1.90, 1.94	1.89, 1.90, 1.91, 1.92	1.90
	Co-O 1.86, 1.88	1.85, 1.87, 1.90, 1.93,	1.85, 1.89, 1.90	1.87, 1.90	

## Bader Charges

Table S4. Calculated Bader charges (q) in e for Sm, B, Co, and O in  $\text{SmB}_x\text{Co}_{1-x}\text{O}_3$ .

<b>B</b>	<b>x=0.125</b>	<b>x=0.25</b>	<b>x=0.5</b>	<b>x=0.75</b>	<b>x=1.00</b>
<b>Mn</b>	q <sub>Sm</sub>	2.06	2.09	2.09	2.08
	q <sub>Mn</sub>	1.74	1.74	1.70	1.68
	q <sub>Co</sub>	1.28	1.25	1.14, 1.35	1.13
	q <sub>O</sub>	-1.15±0.05	-1.17±0.05	-1.19±0.04	-1.19±0.04
<b>Fe</b>	q <sub>Sm</sub>	2.06	2.08	2.05	2.11
	q <sub>Fe</sub>	1.70	1.73	1.71	1.68
	q <sub>Co</sub>	1.28	1.26	1.17	1.18
	q <sub>O</sub>	-1.13±0.03	-1.15±0.06	-1.16, -1.17	-1.22±0.04
<b>Ni</b>	q <sub>Sm</sub>	2.10	2.09	2.06	2.07
	q <sub>Ni</sub>	1.17	1.29	1.27	1.33, 1.12
	q <sub>Co</sub>	1.17, 1.55	1.21, 1.36	1.35	1.31
	q <sub>O</sub>	-1.16±0.04	-1.13±0.03	-1.13±0.04	-1.11±0.03
<b>Cu</b>	q <sub>Sm</sub>	2.02	2.06	2.06	2.07
	q <sub>Cu</sub>	1.32	1.28	1.25	1.18, 1.20
	q <sub>Co</sub>	1.30	1.19, 1.30, 1.53	1.34, 1.24	1.40
	q <sub>O</sub>	-1.10±0.02	-1.13±0.01	-1.11±0.02	-1.11±0.02

## Magnetic Structure of SmBO<sub>3</sub>

Table S5. Difference in total energies of simulation cell between different magnetic structures for SmBO<sub>3</sub> and their related magnetic moment. Note that SmNiO<sub>3</sub> AFM are really ferromagnetic, with different magnetic moments and non-zero total magnetic moment. N/A signifies magnetic structures that were not possible to obtain.

		<b>AAFM</b>	<b>CAFM</b>	<b>FM</b>	<b>GAFM</b>	<b>NM</b>
<b>SmMnO<sub>3</sub></b>	E <sub>diff</sub> (eV)	2.20	N/A	0.00	2.60	N/A
	u <sub>B</sub>	3.82	N/A	3.93	3.82	N/A
<b>SmFeO<sub>3</sub></b>	E <sub>diff</sub> (eV)	1.78	0.00	2.65	0.89	N/A
	u <sub>B</sub>	4.31	4.20	4.40	4.23	N/A
<b>SmNiO<sub>3</sub></b>	E <sub>diff</sub> (eV)	9.57	2.05	0.00	2.65	N/A
	u <sub>B</sub>	1.44-6.15	0.33-1.76	2.05	1.06-2.03	N/A
<b>SmCuO<sub>3</sub></b>	E <sub>diff</sub> (eV)	N/A	N/A	5.26	N/A	0.00
	u <sub>B</sub>	N/A	N/A	0.88	N/A	0.00

## Electronic Conductivity of SmB<sub>x</sub>Co<sub>1-x</sub>O<sub>3</sub>

Table S6. Electrical conductivity,  $\sigma_e$  (Scm<sup>-1</sup>), for SmB<sub>x</sub>Co<sub>1-x</sub>O<sub>3</sub>. Relaxation time set to 0.12 fs.

<b>B</b>	<b>x=0.125</b>	<b>x=0.25</b>	<b>x=0.5</b>	<b>x=0.75</b>	<b>x=1.0</b>
<b>Mn</b>	810	120	90	213	70
<b>Fe</b>	320	0	0	0	0
<b>Ni</b>	10	190	41	20	61
<b>Cu</b>	20	120	100	39	23

## Density of States

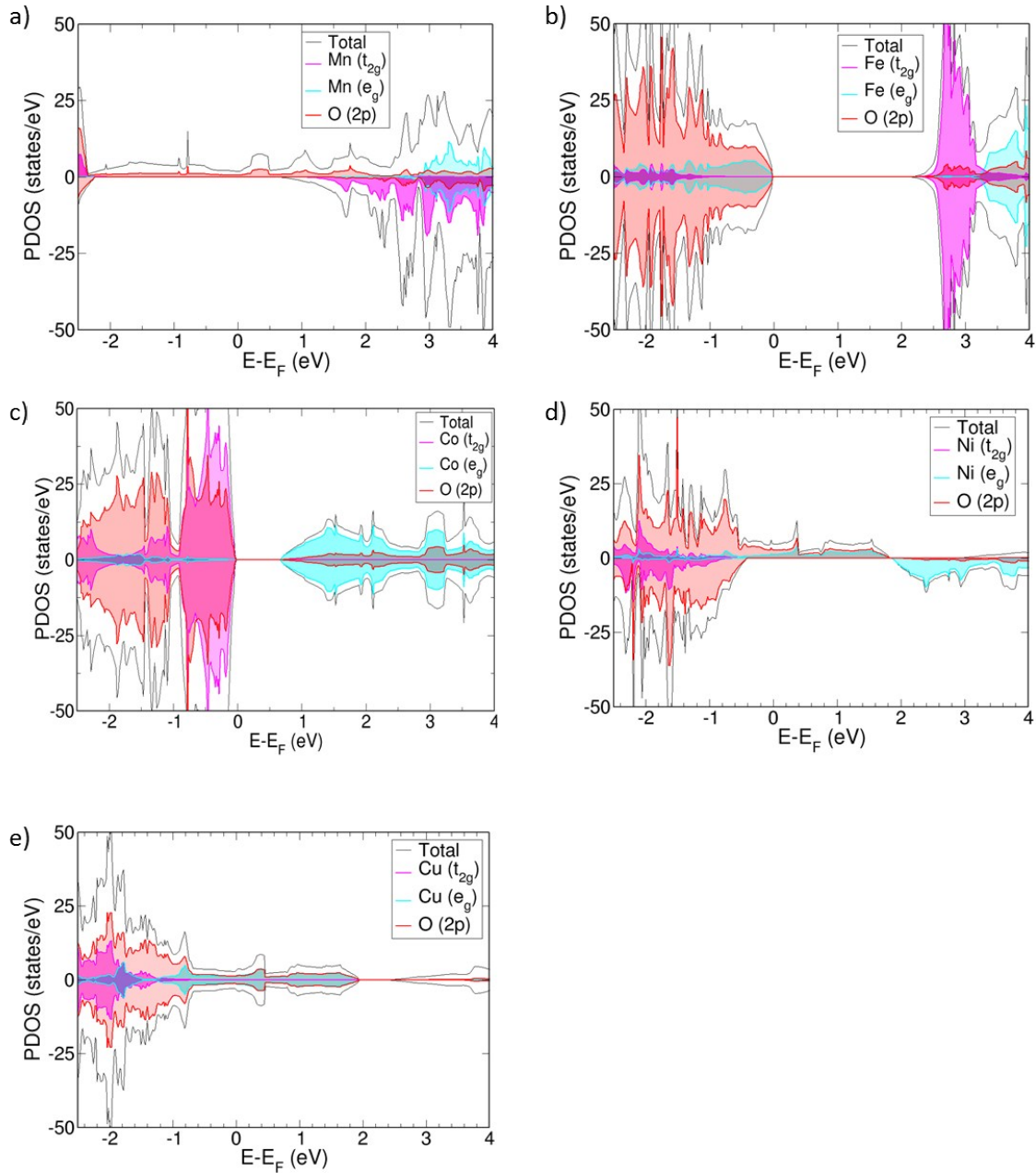


Figure S3. Projected density of states (PDOS) for a) SmMnO<sub>3</sub>, b) SmFeO<sub>3</sub>, c) SmCoO<sub>3</sub>, d) SmNiO<sub>3</sub>, and e) SmCuO<sub>3</sub>.

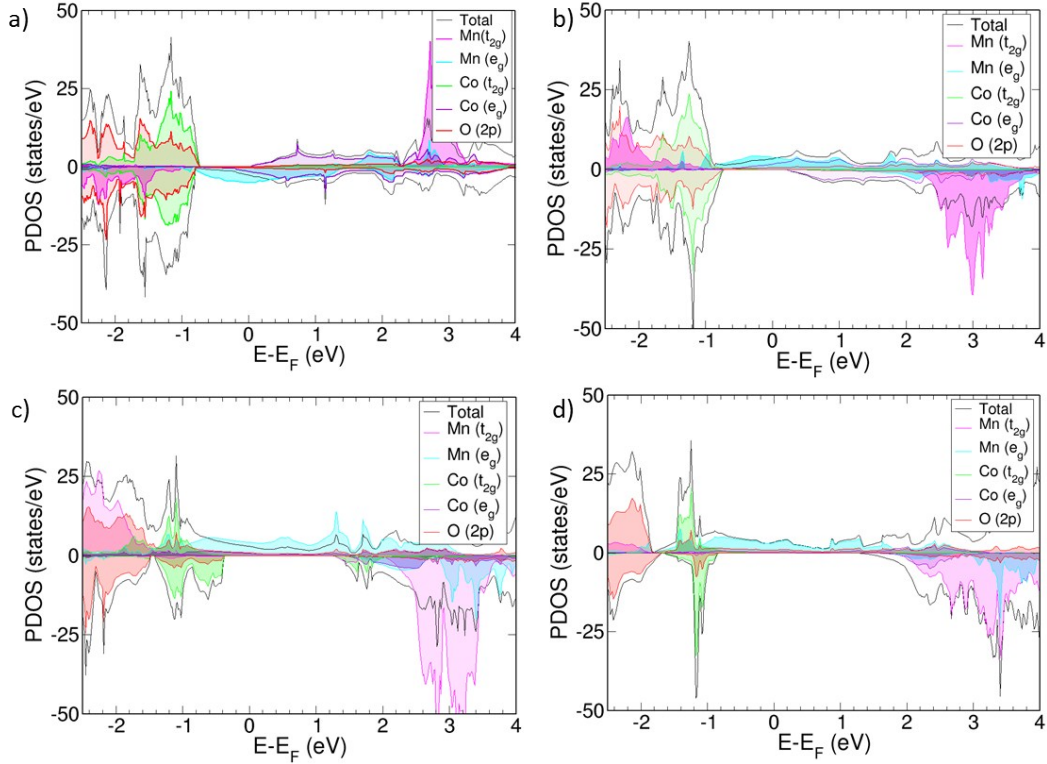


Figure S4. PDOS for a)  $x=0.125$ , b)  $x=0.25$ , c)  $x=0.5$ , and d)  $x=0.75$   $\text{SmCo}_{1-x}\text{Mn}_x\text{O}_3$ . Please note that the Mn PDOS has been multiplied by 10 in a, 5 in b and c, and 2 in d.

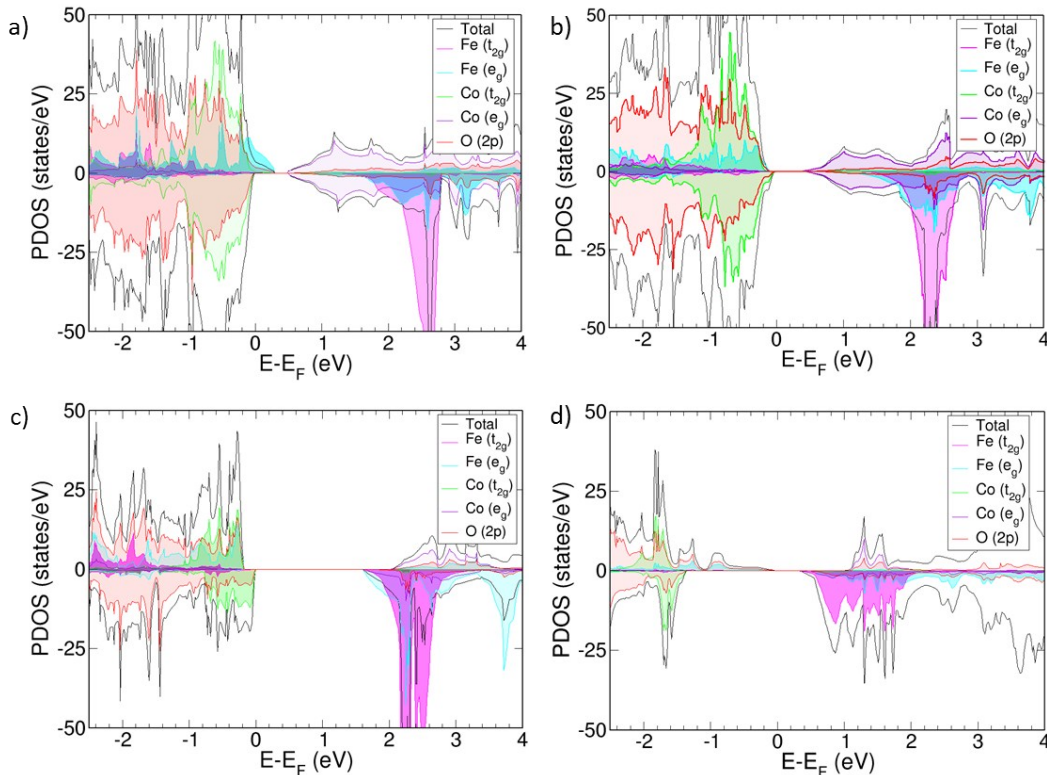


Figure S5. PDOS for a)  $x=0.125$ , b)  $x=0.25$ , c)  $x=0.5$ , and d)  $x=0.75$   $\text{SmCo}_{1-x}\text{Fe}_x\text{O}_3$ . Please note that the Fe PDOS has been multiplied by 10 in a, 5 in b and c, and 2 in d.

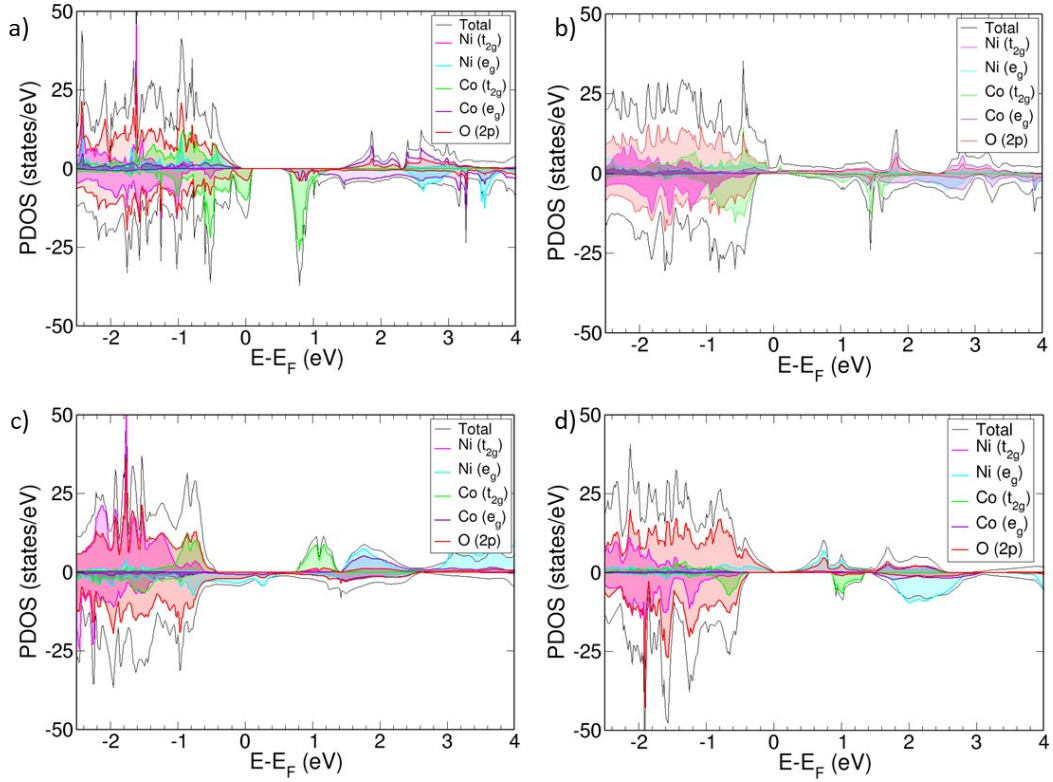


Figure S6. PDOS for a)  $x=0.125$ , b)  $x=0.25$ , c)  $x=0.5$ , and d)  $x=0.75$   $\text{SmCo}_{1-x}\text{Ni}_x\text{O}_3$ . Please note that the Ni PDOS has been multiplied by 10 in a, 5 in b and c, and 2 in d.

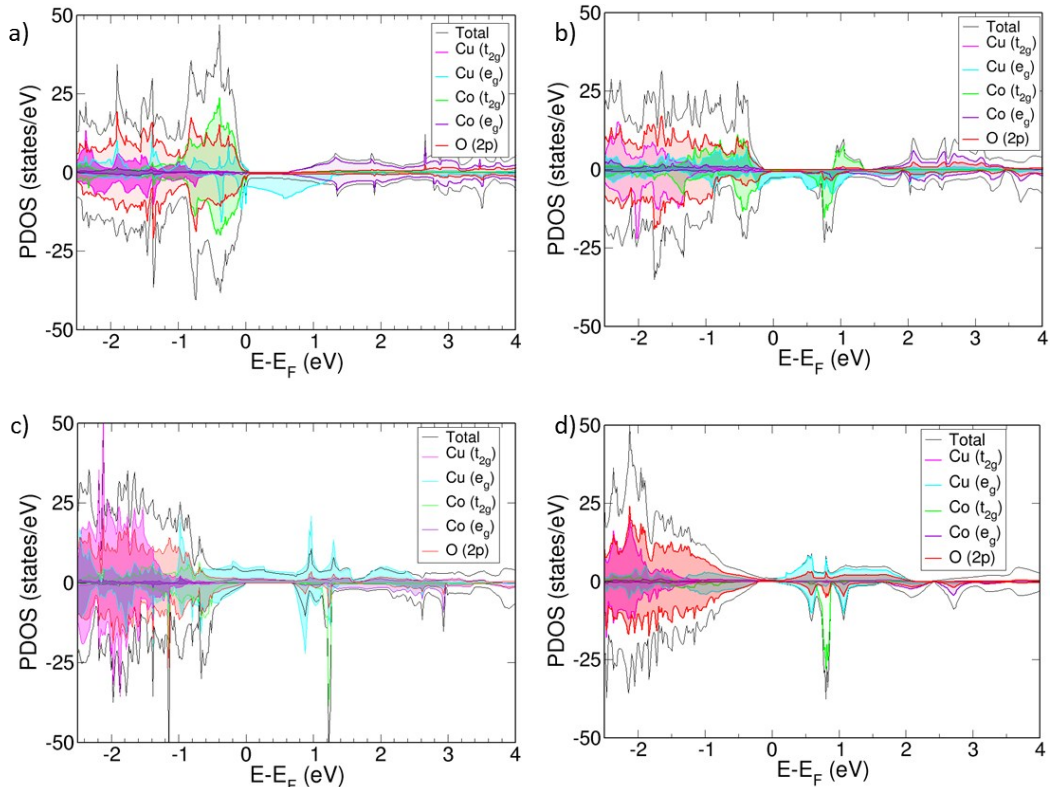


Figure S7. PDOS for a)  $x=0.125$ , b)  $x=0.25$ , c)  $x=0.5$ , and d)  $x=0.75$   $\text{SmCo}_{1-x}\text{Cu}_x\text{O}_3$ . Please note that the Cu PDOS has been multiplied by 10 in a, 5 in b and c, and 2 in d.

### Evaluation of Oxygen Vacancy Position

Table S7. Oxygen vacancy positions and formation energies. N/A signifies no such possible oxygen vacancy position in the lattice. The number of vacancy sites is different in each material and is dependent on the dopant configuration from the bulk calculations.

		<b>x=0.125</b>	<b>x=0.25</b>	<b>x=0.5</b>	<b>x=0.75</b>	<b>x=1.0</b>
<b>SmMn<sub>x</sub>Co<sub>1-x</sub>O<sub>3</sub></b>	Mn-V <sub>O</sub> -Mn	N/A	2.73	2.65	2.70, 2.94	2.36
	Mn-V <sub>O</sub> -Co	3.71	2.76	2.06, 2.14,	3.00, 2.75	N/A
				2.36, 2.47, 2.91		
	Co-V <sub>O</sub> -Co	2.27, 2.56	2.71, 3.21	2.76	N/A	N/A
	Fe-V <sub>O</sub> -Fe	N/A	2.70	N/A	3.31, 3.43	5.65
	Fe-V <sub>O</sub> -Co	2.63	2.94, 2.76	3.53	1.99, 3.32	N/A
<b>SmFe<sub>x</sub>Co<sub>1-x</sub>O<sub>3</sub></b>	Co-V <sub>O</sub> -Co	2.32, 3.05	2.70	N/A	N/A	N/A
	Ni-V <sub>O</sub> -Ni	N/A	1.41	2.48	0.44, 1.43	0.55
	Ni-V <sub>O</sub> -Co	2.76	1.57, 1.79	2.39	0.47, 0.57	N/A
	Co-V <sub>O</sub> -Co	1.66, 1.84	1.09	2.16	N/A	N/A
<b>SmNi<sub>x</sub>Co<sub>1-x</sub>O<sub>3</sub></b>	Cu-V <sub>O</sub> -Cu	N/A	1.43	0.93, 0.96, 1.09	0.62, 0.71	0.54
	Cu-V <sub>O</sub> -Co	2.19	0.55, 0.70	0.79, 0.81, 0.86, 1.22	0.42, 0.52	N/A
	Co-V <sub>O</sub> -Co	2.20, 2.65	0.92	1.29, 1.36, 1.44	N/A	N/A

## Thermal Expansion Coefficients

Table S8. Thermal expansion coefficients (TEC) in  $\times 10^{-6} \text{ K}^{-1}$  for  $\text{SmB}_x\text{Co}_{1-x}\text{O}_3$ . TEC have been calculated over a temperature range of 600-1200K.

B	x=0.125	x=0.25	x=0.5	x=0.75	x=1.0
<b>Mn</b>	15.6	16.9	17.7	14.9	15.5
<b>Fe</b>	18.1	17.5	17.0	17.2	16.9
<b>Ni</b>	16.1	17.3	17.6	16.7	16.1
<b>Cu</b>	17.3	17.4	18.6	15.8	14.2

## References

- <sup>1</sup> E. Olsson, X. Aparicio-Anglès, and N.H. de Leeuw, Phys. Chem. Chem. Phys. **19**, 13960 (2017).
- <sup>2</sup> M. Cherry, M.S. Islam, and C.R.A. Catlow, J. Solid State Chem. **118**, 125 (1995).
- <sup>3</sup> P.G. Sundell, M.E. Björketun, and G. Wahnström, Phys. Rev. B **73**, 104112 (2006).
- <sup>4</sup> E. Olsson, X. Aparicio-Anglès, and N.H. de Leeuw, J. Chem. Phys. **145**, 014703 (2016).